

# ON THE RELATIVE CONTRIBUTIONS OF ABSORPTION AND SCATTERING TO ULTRASOUND ATTENUATION IN TRABECULAR BONE: A SIMULATION STUDY

Jonathan J. Kaufman<sup>\*a,b</sup>, Gangming Luo<sup>c</sup>, and Robert S. Siffert<sup>a</sup>

<sup>a</sup>Department of Orthopaedics, The Mount Sinai School of Medicine, New York, NY

<sup>b</sup>CyberLogic, Inc., New York, NY

<sup>c</sup>New York Department of Veterans Affairs Medical Center & Department of Rehabilitation Medicine and the New York University Medical Center, New York, NY

*Abstract* - Ultrasound has been proposed as a means to non-invasively assess bone and particularly bone strength and fracture risk. Although there has been some success in this application, there is still much that is unknown regarding the propagation of ultrasound through bone. Because strength and fracture risk are a function of both bone mineral density as well as architectural structure and tissue quality, this study was carried out to further elucidate the mechanisms of interaction between ultrasound and bone. Frequency-dependent attenuation of an ultrasound wave in trabecular bone has been shown to be strongly dependent on bone mass and architecture and is currently used in several clinical devices for bone assessment. Since attenuation is due to both absorption by the biological tissues *per se* and scattering, it is of interest to understand the relative contributions of each. A sample of calcaneal trabecular bone was scanned with micro-CT and subjected to morphological image processing (erosions and dilations) to obtain a total of 11 three-dimensional (3D) data sets. Eleven two-dimensional (2D) slices obtained from the 3D data sets were then analyzed to evaluate their bone volume fractions (VF). Computer simulations of ultrasonic propagation through each of the 11 2D bone slices, which varied in VF from 0.088 - 0.181, were carried out in one of two modes. In the first instance, the component tissues (i.e., marrow and bone) were lossy, while in the second set of simulations the component tissues were lossless. In both cases the slope of the attenuation was computed over the frequency range 300 kHz - 900 kHz for the entire data set. Results obtained showed an average reduction in the attenuation slope of only 4.4% (SD=1.8%) in the lossless case as compared (pairwise) with the lossy case. This data indicates that scattering is the primary mechanism in trabecular bone with respect to overall attenuation

measurements, and further suggests that models relating scattering to bone architecture and mass should be developed to further enhance the ability of ultrasound to non-invasively assess bone.

## I. INTRODUCTION

Ultrasound is currently being investigated as a means for non-invasively assessing bone. It has been suggested since ultrasound is a mechanical wave that it may be able to evaluate additional factors related to bone strength in comparison to bone density alone [1]. For example, it is known that architectural structure is an important aspect in osteoporotic fractures [2], although the primary method currently used for clinical bone assessment is based on x-ray absorptiometry, which measures total bone mass and is insensitive to architectural changes [3]. Although ultrasonic methods appear promising, they have not yet fulfilled their potential and much is still unknown about how ultrasound interacts with bone. The aim of this study is to elucidate one aspect of that interaction, namely to examine the relative contributions of tissue absorption and scattering to frequency-dependent attenuation (FDA). FDA is a widely used parameter for assessing bone, although at present there is not a great deal of understanding as to what properties of bone it is measuring. The information provided here should help in developing models which relate ultrasonic parameters like FDA to the underlying biophysical properties of bone, such as its mass and microarchitecture, and ultimately it is hoped, to fracture risk. A second objective of the study is to demonstrate to the scientific and engineering community the usefulness of computational methods in furthering research and

development in tissue and bone characterization in particular and in ultrasound in general.

## II. MATERIALS AND METHODS

A human calcaneus was obtained from a commercial supplier from which all soft tissue had been previously removed. A cylindrical core 1.42 cm in diameter was cut from the posterior portion of the calcaneus in the medial-lateral direction, using an electric drill corer. The cortical shells were then removed using a rotating diskcutter to produce a 10.3 mm long cylindrical sample of calcaneal trabecular bone. The specimen was three-dimensionally imaged using micro-CT and the data reconstructed in cubic volume elements (voxels) that were 33.4 microns ( $\mu$ ) on edge.

The 3D image data corresponding to the trabecular bone cylinder was then processed using sequences of morphologic image processing operations [4]. The processes of erosion (thinning) and dilation (thickening) were applied in various combinations to obtain bone images in distinct states of densities and architectures. In particular, the original image data was eroded and dilated in 10 distinct erosion and dilation sequences to obtain a total of 11 distinct 3D images. The distinct sequences of erosions and dilations were chosen so that the changes induced on the original specimen might mimic those seen under osteoporosis [4]. An arbitrarily selected 2D slice was then extracted from each of the 11 3D data sets to obtain a total of 11 2D images. Each of the 11 2D images was then analyzed for volume fraction, defined as the proportion of the total image area occupied by bone, and thus varied between zero and one. It is directly analogous to bone mineral density, apart from a constant scale factor.

Next, computer simulations of ultrasound propagation through each of the 11 2D images were carried out using a computer software package (*Wave2000 Pro*, CyberLogic, Inc., New York, NY). *Wave2000 Pro* simulates the complete solution to the two-dimensional viscoelastic wave equation [5]:

$$\rho \frac{\partial^2 w}{\partial t^2} = (\mu + \eta \frac{\partial}{\partial t}) \nabla^2 w + (\lambda + \mu + \xi \frac{\partial}{\partial t} + \frac{\eta}{3} \frac{\partial}{\partial t}) \nabla (\nabla \cdot w) \quad (1)$$

In Eq. (1),  $\rho$  is the volumetric density in  $\text{kg/m}^3$  of each material *per se*,  $\lambda$  and  $\mu$  are the first and second Lamé constants, respectively, in units of  $\text{N/m}^2$ ,  $\eta$  and  $\xi$  are the first and second viscosities in units of  $\text{N-s/m}^2$ , and  $w = w(x,y,t)$  is the displacement vector as a function of Cartesian coordinates  $x$  and  $y$  and of time  $t$ . *Wave2000 Pro* implements a finite difference time domain solution to Eq. (1), and is based on a local interaction formulation designed for parallel processing implementation, as presented in [6] for the lossless case. *Wave2000 Pro* implements an extension of this formulation, which allows for viscous absorption losses and execution on a standard PC running Microsoft Windows 95 and higher.

The simulations were carried out in one of two modes. In the first mode, the component tissues (i.e., marrow and bone) were lossy and had the following parameters. For the bone portions of the interrogated sample,  $\rho = 1850 \text{ kg/m}^3$ ,  $\lambda = 9306 \text{ MPa}$ ,  $\mu = 3127 \text{ MPa}$ ,  $\eta = 100 \text{ Pa} \cdot \text{s}$ ,  $\xi = 0.1 \text{ Pa} \cdot \text{s}$ . This produced longitudinal and shear (phase) velocities at 1 MHz of 2903 m/s and 1320 m/s, and differential specific attenuations of 10.1 dB/cm/MHz and 80.3 dB/cm/MHz, respectively. The material in the marrow spaces of the tissue was assumed to be fresh blood. For this case,  $\rho = 1055 \text{ kg/m}^3$ ,  $\lambda = 2634 \text{ MPa}$ ,  $\mu = 0 \text{ MPa}$ ,  $\eta = 1.0 \text{ Pa} \cdot \text{s}$ ,  $\xi \approx 0 \text{ Pa} \cdot \text{s}$ . This produced longitudinal and shear (phase) velocities at 1 MHz of 1580 m/s and 109 m/s, and differential specific attenuations of 1.1 dB/cm/MHz and 2500 dB/cm/MHz, respectively.

In the second mode, the simulations were obtained with all viscous loss terms set to zero. This resulted in attenuations of zero for both the bone and blood component tissues. The phase velocities were not affected significantly from those given above by setting the viscous loss parameters to zero.

A 1 MHz sine wave with a Gaussian envelope was used as the source waveform in all cases. The source and receiver were operated in through transmission mode; each was 10.32 mm long and extended over the entire respective opposite sides of the 2D image, with propagation in the medial-lateral direction. The receiver computed the average or mean displacement along its defined length. Finally, the slope of the frequency dependent attenuation was computed over the frequency range 300 kHz - 900 kHz for each sample in both the lossy and lossless modes.

### III. Results

Fig. 2 displays the receivers' outputs for a simulation of the sample shown in Fig. 1, with and without tissue absorption. Fig. 3 shows a "snapshot" in time of the propagating wave at  $t=8.5$  microseconds (with absorption). As maybe seen, there is a distinct ballistic component followed by what appears to be a scattered field. The actual frequency-dependent attenuation curves for two samples are shown in Fig. 4 ( $VF=0.17$ ) and Fig. 5 ( $VF=0.09$ ), again with and without absorption. As maybe seen, there is only a small decrease in attenuation in the absorption-free case. Fig. 6 displays the slope of the FDA as a function of volume fraction, again showing a small decrease in slope in the lossless case. Pairing the data (lossy and lossless) and evaluating the percent change, the overall average (SD) decrease is 4.4% (1.8%) in the value of attenuation slope for the lossless case as compared to the attenuation slopes for the lossy case.

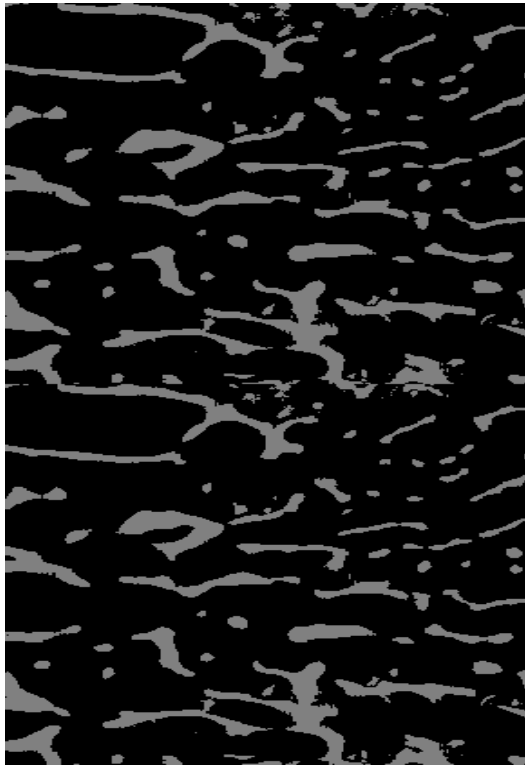


Fig. 1. A slice of the original micro-CT, in the medial-lateral direction (top-to-bottom, respectively), with  $VF=0.17$ .

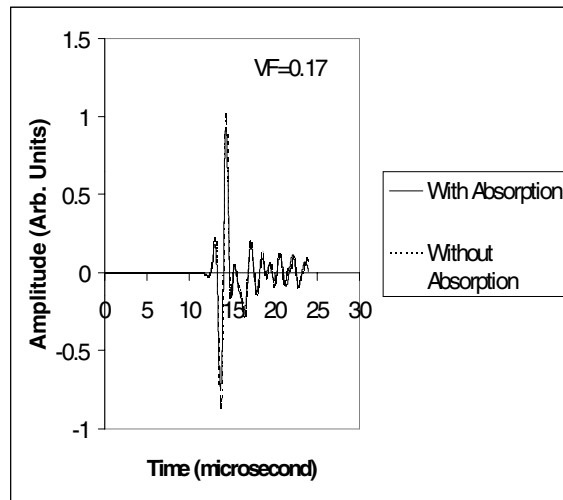


Fig. 2. Received waveforms for the bone slice as shown in Fig. 1 (below left), with and without absorption.

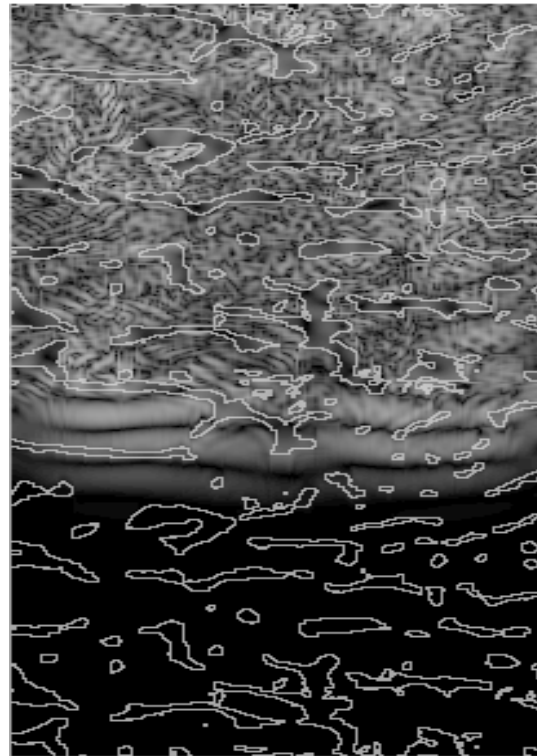


Fig. 3. "Snapshot" of displacement magnitude at  $t = 8.522$  microseconds. Note the apparent "ballistic wave" followed by what appears to be a scattered wave.

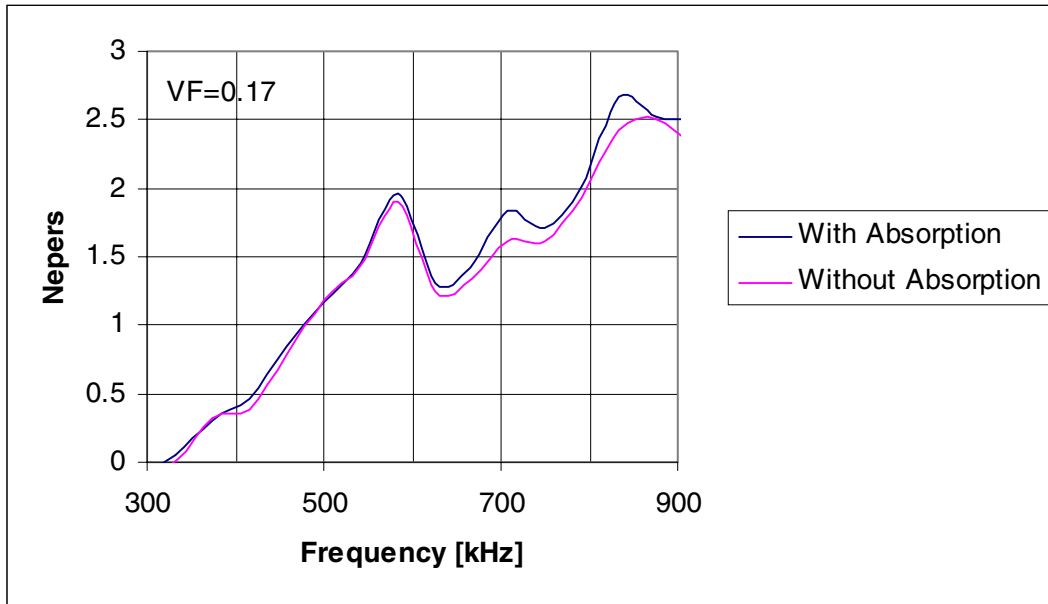


Fig. 4. Frequency-dependent attenuations for the bone slice of Fig. 1, with and without absorption.

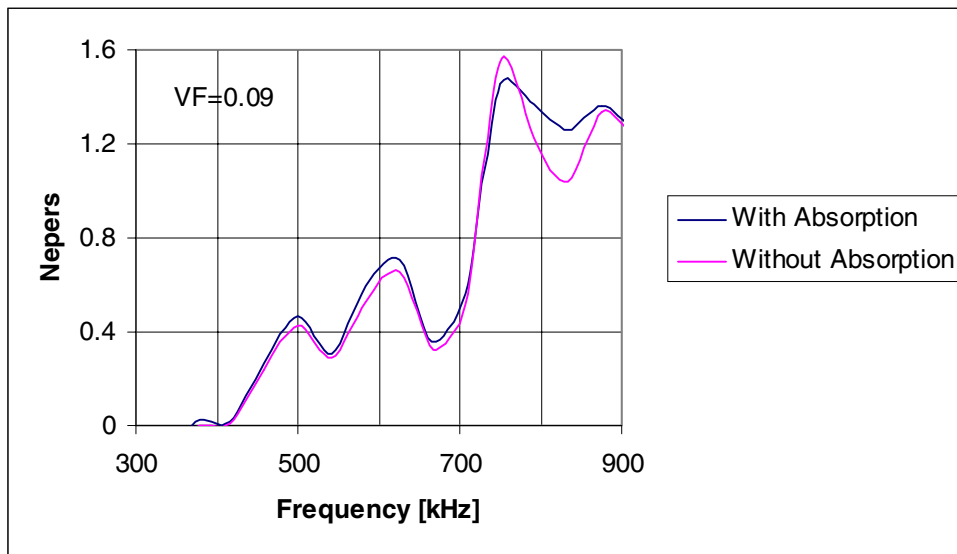


Fig. 5. Frequency-dependent attenuations for another bone slice having a  $VF = 0.09$ , with and without absorption.

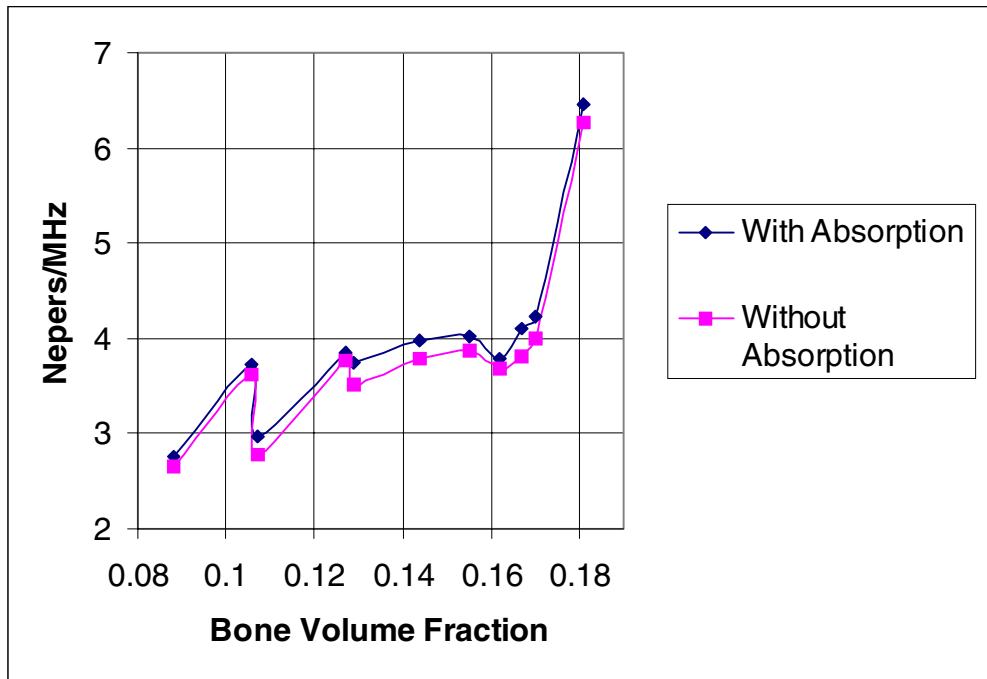


Fig. 6. The slopes of the frequency-dependent attenuation as a function of VF for the case of lossy and lossless tissues in trabecular bone.

#### IV. DISCUSSION & CONCLUSION

This paper has demonstrated that most of the frequency dependent attenuation observed in trabecular bone is due to scattering of the ultrasound wave and not from absorption losses *per se*. This is somewhat surprising in view of the significant amount of absorption loss of bone tissue (i.e., about 10 dB/cm/MHz); apparently this is because of the very small amount of bone tissue present (the maximum VF in this study was 0.18) and thus compared to the large degree of scattering was relatively small in comparison. Although this must be verified by analysis and experimentation, these results would point to further development of new scattering models (such as in [7, 8]) relating attenuation and scattering to bone density and architecture and ultimately to fracture risk.

#### V. REFERENCES

- [1] JJ Kaufman et al., Review - Ultrasound Assessment of Bone, *J Bone Min Research*, 8(5), pp. 517-525, 1993.  
 [2] AM Parfitt, Trabecular Bone Architecture in the Pathogenesis and Prevention of Fracture, *Am J Med*,

82(1B), pp.68-72, 1987.

- [3] SM Ott, RF Kilcoyne, C Chestnut III, Ability of Four Different Techniques of Measuring Bone Mass to Diagnose Vertebral Fractures in Postmenopausal Women, *J Bone Min Research*, 2, pp. 201-210, 1987.  
 [4] GM Luo, JH Kinney, JJ Kaufman, D Haupt, A Chiabrera, RS Siffert, Relationship of Plain Radiographic Patterns to 3D Trabecular Architecture in the Human Calcaneus, *Osteoporosis Int*, 9(4), pp. 339-345, 1999.  
 [5] GM Luo, JJ Kaufman, A Chiabrera et al., Computational Methods for Ultrasonic Bone Assessment, *Ultrasound in Medicine and Biology*, 25, pp. 823-830, 1999.  
 [6] PP Delsanto, RS Schechter, HH Chaslekis et al., Connection Machine Simulation of Ultrasonic Wave Propagation in Materials. ii: The Two-Dimensional Case, *Wave Motion*, 20, pp. 295-303, 1994.  
 [7] F Jenson, F Padilla, P Laugier, Prediction of Frequency Dependent Ultrasonic Backscatter in Cancellous Bone Using Statistical Weak Scattering Model, *Ultrasound in Med. & Biol.*, 29(3), pp. 455-464, 2003.  
 [8] KA Wear, Frequency Dependence of Ultrasonic Backscatter from Human Trabecular Bone: Theory and Experiment, *J Acoust Soc Am*, 106(7), pp. 3659-3664, 1999.

\*Jonathan J. Kaufman e-mail: jkk Kaufman@cyberlogic.org

**Acknowledgment:** This work was supported in part by The Carroll and Milton Petrie Foundation, and by SBIR Grant #2R44 AR45150 from NIAMS of the NIH.